# Quench Performance of a Large-Aperture Nb<sub>3</sub>Sn Cos-theta Coil with Stress Management in Dipole Mirror Configurations

A.V. Zlobin, I. Novitski, M. Baldini, and E. Barzi, Senior Member, IEEE

Abstract—A 123-mm aperture Nb<sub>3</sub>Sn cos-theta (CT) dipole coil with Stress Management (SM) has been developed at Fermilab to demonstrate and test the SM concept including coil design, fabrication technology and performance. The first SMCT1 coil has been fabricated and assembled together with a 60-mm aperture Nb<sub>3</sub>Sn coil inside a dipole mirror structure and tested separately and in series with the inner coil. This paper summarizes the design, parameters, and quench performance of the SMCT1 coil in a dipole mirror configuration.

Index Terms— Accelerator magnet, dipole mirror, magnetic field, mechanical structure, Rutherford cable, stress management.

# I. INTRODUCTION

N innovative stress management (SM) concept for costheta (CT) coils (SMCT coil concept) has been proposed and is being developed and studied at Fermilab [1], [2]. The first 123-mm aperture 2-layer Nb<sub>3</sub>Sn SMCT dipole coil (SMCT1) was developed and fabricated to validate and test the SM concept including coil design, fabrication technology, and performance. The coil was assembled and tested with a 60-mm aperture 2-layer Nb<sub>3</sub>Sn coil (MDP03), previously tested in MDPCT1 dipole [3], [4] using a dipole mirror structure. This approach allows coil testing under operating conditions similar to those of real magnets [5]. It was widely used at Fermilab to develop Nb<sub>3</sub>Sn coil technologies, including technology scale up, and conductor stability and quench protection studies [6]-[8].

SMCT1 coil testing in a dipole mirror structure was done in two configurations - SMCTM1a with powering the SMCT1 coil only, and SMCTM1b with powering the SMCT1 coil in series with the MDP03 coil. The objective of the tests was to prove the SMCT coil concept in 2-layer and 4-layer mirror configurations; demonstrate that the magnet can reach the target current (coil field) at the established preload; study magnet training, training memory after thermal cycle, ramp rate and temperature dependences of the magnet quench current.

This paper briefly describes the SMCT1 coil and dipole mirror designs and parameters (more details are in [9]-[11]). The results of quench performance studies of SMCTM1a and SMCTM1b dipole mirror magnets are presented and discussed.

### II. SMCT COIL DESIGN AND TEST CONFIGURATIONS

A cross-section and 3D view of the 123-mm aperture and 206-mm outer diameter SMCT1 dipole coil with transverse and longitudinal cuts at the coil "return" end are shown in Fig. 1. The SMCT1 coil consists of 2-layers. The turns in each layer are combined in 5 blocks wound into a 316L stainless-steel mandrel with 5 mm radial and azimuthal block separation [9]. To produce a dipole field in the magnet aperture, the number of turns in the blocks approximately follows the cos-theta distribution. The SMCT1 coil mandrel has a complex 3D geometry. It was manufactured using advanced Additive Manufacturing technology [10].

The SMCT1 coil uses 40-strand Rutherford cable with a width of 15.1 mm, a mid-thickness of 1.319 mm and a keystone angle of 0.805 degree. The cable is made of a Nb<sub>3</sub>Sn composite wire 0.7 mm in diameter with a Cu/nonCu ratio of 1.13 and  $J_c$  at 15 T and 4.2 K of 1500 A/mm<sup>2</sup> [11]. The strand and cable cross-sections are shown in Fig. 1.

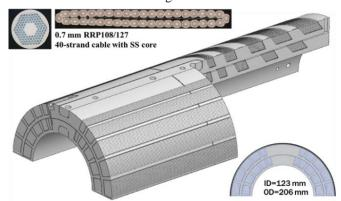


**Fig. 1.** Nb<sub>3</sub>Sn strand and cable cross-sections (top left), 3D-view (middle) and cross-section (bottom right) of the 123-mm aperture two-layer SMCT1 coil.

A 3D view of the 4-layer coil assembly in a dipole mirror structure is shown in Fig. 2. The coil assembly, surrounded by a 1 mm thick 316L stainless steel shell, was installed inside the bottom part of the horizontally split iron yoke. The yoke is made of AISI 1020 iron laminations with an outer diameter of 587 mm, connected by 7075-T6 Aluminum I-clamps, and enclosed in a 12.5 mm thick 316 stainless-steel skin. The coil ends are supported by two independent systems. The SMCT1 coil is supported by eight 24.5 mm diameter rods and 50 mm thick end plates. The MDP03 coil is supported by four 30 mm diameter rods and two end plates that are 50 mm thick inside and 30 mm thick outside.

<sup>\*</sup> Work supported by Fermi Research Alliance, LLC, under contract No. DE-AC02-07CH11359 with the U.S. DOE and US MDP. Authors are with the Fermi National Accelerator Laboratory (FNAL), Batavia, IL 60510 USA (e-mail: zlobin@fnal.gov).

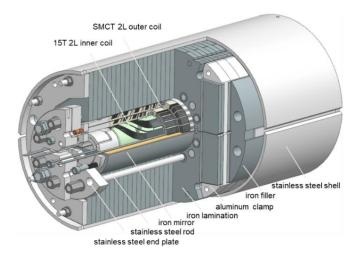


Fig. 2. 3D view of the 4-layer dipole mirror magnet.

The coil preload during assembly was applied by shims placed in the coil midplane, in-between the two coils, between the coil and the iron yoke, and between the yoke and the skin, as well as by the yoke-clamp interference and skin tension after welding. During cool-down to LHe temperatures, the coil stress is controlled by the horizontal gap between yoke top and bottom blocks. The maximum stress estimated using ANSYS, in the inner MDP03 coil after assembly is less than 130 MPa and in SMCT1 coil it is less than 50 MPa. After cool-down the maximum stress in the MDP03 coil increases to 173 MPa and in SMCT1 coil to ~80 MPa. With Lorentz forces, the highest coil stresses at a coil  $B_{max}$  of 13 T in 2-layer configuration and at a  $B_{max}$  of 15 T in 4-layer configuration are in the MDP03 coil on the level of 160-170 MPa [12]. The maximum stress in MDP03 coil is close to the limit for Nb<sub>3</sub>Sn cables.

## III. SMCT1 COIL TEST

The SMCTM1 test was done in two configurations with the SMCT1 coil first powered independently (2-layer configuration SMCTM1a) and then in series with the inner coil MDP03 (4-layer configuration SMCTM1b).

Traditionally, magnet quench performance is represented by the quench current  $I_q$ . In this paper, quench data are reported as the maximum field  $B_{max}$  in the corresponding coil. Using  $B_{max}$  allows comparing quench performance of the SMCT1 coil in the two described mirror configurations. It is also suited for comparing the quench performance of SMCTM1b mirror with that of the 4-layer dipole MDPCT1, which used similar mechanical structure and inner coils, but with outer coils without coil stress management [3], [4]. Moreover, the coil  $B_{max}$  allows also to estimate the performance of the SMCT1 coil in the dipole configuration.

Conductor limits of SMCT1 and MDP03 coils in 2-layer and 4-layer dipole mirrors at 1.9 K and 4.5 K, as calculated using witness sample data with self-field correction, are summarized in Table I. In SMCTM1a, the  $B_{max}$  limits of SMCT1 coil at 1.9 K and 4.5 K are 14.2 T and 13.1 T respectively. They are reached at the coil  $I_{SSL}$  current of 16.5 kA and 14.8 kA respectively [13].

TABLE I
CONDUCTOR LIMITS OF SMCT1 AND MDP03 COILS IN 2-LAYER AND 4-LAYER
DIPOLE MIRRORS AT 1.9 K AND 4.5 K

Differentiations in 15 11 in 12					
Magnet	Coil	1.9 K		4.5 K	
		I <sub>SSL</sub> , kA	$B_{max}$ , T	I <sub>SSL</sub> , kA	$B_{max}$ , T
SMCTM1a	SMCT1	16.47	14.21	14.89	13.04
SMCTM1b -	SMCT1	14.06	15.01	12.69	13.76
	MDP03	14.25	17.4	12.73	15.81

In SMCTM1b, the  $B_{max}$  limits of SMCT1/MDP03 coils at 1.9 K and 4.5 K are 15.0/17.4 T and 13.8/15.8 T obtained at coil currents of 14.06/14.25 kA and 12.69/12.73 kA respectively. One can notice that the  $I_{SSL}$  of SMCT1 and MDP03 coils in the 4-layer SMCTM1b are very close. At 1.9 K the  $I_{SSL}$  of MDP03 coil is only 1.3% lower than the  $I_{SSL}$  of SMCT1 coil which is within the accuracy of the  $I_{SSL}$  calculation. At 4.5 K this difference is less than 0.5%. Although the conductor  $B_{max}$  limits of 4-layer SMCTM1b at 1.9 K and 4.5 K are rather high, 17.4 T and 15.8 T respectively, the actual magnet  $B_{max}$  limit is 15 T at both temperatures since it is determined by the maximum mechanical stress in MDP03 coil [12].

# A. SMCTM1a Test

The SMCTM1a test started with magnet training followed by quench current ramp rate studies at 1.9 K and temperature dependence measurements in a temperature range of 1.9-4.5 K. After a thermal cycle (TC) to room temperature, measurements of magnet training, ramp rate and temperature dependences were repeated at 1.9 K [13].

The SMCTM1a training data at 1.9 K before and after TC are summarized in Fig. 3. The tests were performed at a current ramp rate of 20 A/s. SMCT1 coil training began at a coil  $B_{max}$  of 10.6 T, which is 70% of the coil short sample limit (SSL) at 1.9 K. After 26 training quenches, the  $B_{max}$  in SMCT1 coil reached 12.7 T (89% of coil SSL). All quenches were detected in the inner layer of the SMCT1 coil except for the first quench that started in the outer-layer middle block, and three other quenches which were detected in the pole block of the coil outer layer. Due to losing the voltage taps (VTs) on coil blocks in the inner layer, the exact location of the quench origin in the inner layer of SMCT1 coil could not be identified.

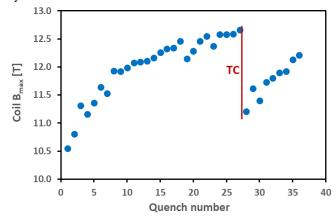


Fig. 3. SMCT1 coil  $B_{max}$  vs. quench number measured at 20 A/s and 1.9 K in SMCTM1a.

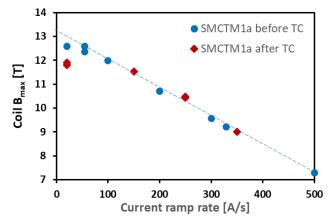


Fig. 4. SMCT1 coil  $B_{max}$  vs. current ramp rate at 1.9 K measured in SMCTM1a before and after TC.

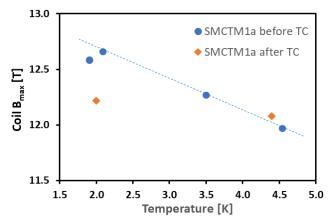


Fig. 5. SMCT1 coil  $B_{max}$  vs. temperature at 20 A/s measured in SMCTM1a before and after TC.

The 1<sup>st</sup> quench after TC was at a coil  $B_{max}$  of 11.2 T. It was slightly higher than the first training quench but well below the  $B_{max}$  before TC, which shows rather poor training memory of the coil. All the quenches after TC were detected in the coil inner layer. Due to a slow training rate, it was decided to stop magnet training after nine quenches.

The SMCT1 coil degradation was estimated using ramp rate and temperature dependences of the coil  $B_{max}$ , shown in Figs. 4 and 5, as measured before and after TC.

The ramp rate dependence of the SMCT1 coil  $B_{max}$  shows linear reduction of the coil quench current with increasing current ramp rate. At a dI/dt of 50 A/s and higher,  $B_{max}$  linearly decreases with increasing current ramp rate. This indicates that the coil ramp rate dependence is determined by the hysteresis loss in the superconducting sub-elements. The other two AC loss components related to eddy currents inside strands and between strands in a cable are relatively small. Linear extrapolation of the coil  $B_{max}$  to dI/dt=0 gives a maximum  $B_{max}$  of 13.1 T, which is 91% of the expected SSL at 1.9 K.

The temperature dependence of  $B_{max}$  in the SMCT1 coil, as measured before TC, shows linear  $B_{max}$  reduction from 12.7 T to 12.0 T, which corresponds to 90% of the conductor limit at 4.5 K. The  $B_{max}$  reached during magnet training at 20 A/s after TC indicates that the training was not completed.

The  $\sim$ 9% reduction of the coil  $B_{max}$  with respect to the SSL at both 1.9 K and 4.5 K is likely due to conductor degradation during SMCT1 coil fabrication and mirror magnet assembly.

The causes are being analysed and will be resolved in the next coils. Although the magnet training after TC was not completed, the consistency of the coil  $B_{max}$  value at ramp rates above 150 A/s and the  $B_{max}$  value itself at ~4.5 K in the SMCTM1a configuration before and after TC confirms that the coil has not degraded during TC including magnet warming up to room temperature and subsequent cooling down to 1.9 K.

# B. SMCTM1b Test

After warming up and reconfiguring the coil connection, the dipole mirror, now called SMCTM1b, was cooled down and the test continued. The test plan included magnet training and ramp rate dependence studies at 1.9 K and temperature dependence measurements between 1.8 and 4.5 K [14]. Quench protection studies with quench heaters, and coil RRR measurements were also performed and will be reported separately.

The SMCT1 and MDP03 coil  $B_{max}$  vs. quench number during SMCTM1b training at 1.9 K is shown in Fig. 6. Six power supply (PS) trips occurred before the first actual quench, and a few PS trips were recorded during magnet training. They are not shown in the plot. The presence of voltage spikes (VSs) in the test points to some mechanical disturbances in the magnet structure. As a possible mechanism, stick/slip axial coil motion due to the separate axial support of MDP03 and SMCT1 coil is considered.

A training plateau was reached after eight quenches. The quenches occurred in both coils; in Figs. 6-8, solid markers indicate the coil where the quench originated. The first quench started in the inner MDP03 coil whereas the second quench was detected with VSs in both coils. The first quenches in SMCT1 coil occurred at a  $B_{max}$  of ~12 T, which is only slightly higher than in SMCTM1a after TC. The  $B_{max}$ , reached in SMCT1 and MDP03 coils at 1.9 K, was 12.6 T and 14.5 T respectively. The  $B_{max}$  at 1.9 K is close to the MDP03 mechanical limit of 15 T.

The dependences of  $B_{max}$  in MDP03 and SMCT1 coils on the current ramp rate measured in SMCTM1b at 1.9 K are shown in Fig. 7. Similar to magnet training, some quenches with VSs occurred in both coils. As in SMCTM1a, at high ramp rates they are well approximated by linear functions. Linear extrapolation of the coil quench field to zero ramp rate based on high ramp rate data gives a  $B_{max}$  value of ~15 T in MDP03 coil and of ~13.1 T in SMCT1 coil at 1.9 K.

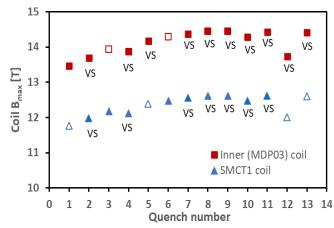


**Fig. 6.**  $B_{max}$  of MDP03 and SMCT1coils vs. quench number measured at 20 A/s and 1.9 K in the SMCTM1b. Solid markers indicate the coil where the quench originated.

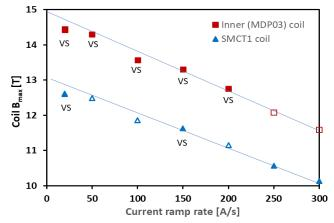


**Fig. 7.**  $B_{max}$  of MDP03 and SMCT1 coils vs. current ramp rate at 1.9 K in SMCTM1b. Solid markers indicate the coil where the quench originated.

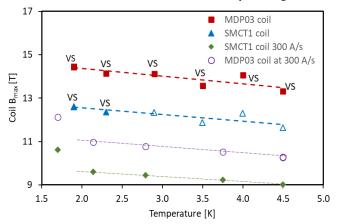


**Fig. 8.** B<sub>max</sub> of MDP03 and SMCT1 coils vs. temperature in SMCTM1b at *dl/dt* of 20 and 300 A/s. Solid markers indicate the coil where the quench originated.

The data for the SMCT1 coil in Fig. 7 are in a good agreement with those shown in Fig. 4 at the same dB/dt values. A  $B_{max}$  value of 14.5 T reached in MDP03 coil during training at 20 A/s indicates that the training was completed with a  $B_{max}$  slightly lower than the conductor limit.

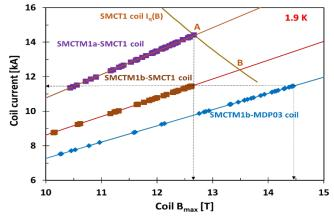
The  $B_{max}$  of MDP03 and SMCT1 coils in SMCTM1b vs. coil temperature, as measured at 20 and 300 A/s, are shown in Fig. 8. The 20 A/s quenches at T<2.5 K were detected in both coils with VSs, whereas above 3 K the quenches were only in the inner coil with VSs. In the temperature range of 1.9-4.5 K, the  $B_{max}$  reduces from 14.5 T to 13.3 T in MDP03 coil, and from 12.6 T to 11.6 T in SMCT1 coil. The larger spread of data points at T>3 K, seen in the plot, could be also attributed to mechanical disturbances in the magnet structure.

All the quenches at 300 A/s were detected in SMCT1 coil without VSs. The 300 A/s data for both coils are ~3 T lower than the quenches at 20 A/s, in agreement with the data in Figs. 4 and 7. The high values of quench currents at 1.7 K in Fig. 8 could be explained by better coil cooling in superfluid helium.

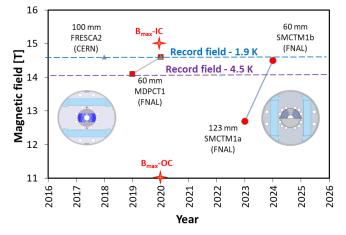
# IV. DISCUSSION

Figure 9 shows  $B_{max}/I$  load lines (LL) for the SMCT1 coil in SMCTM1a, and for MDP03 and SMCT1 coils in SMCTM1b. The points on the load lines represent all the quench data shown

in Figs. 4-8. The  $I_q(B)$  curve represents the field dependence of the coil quench current at dI/dt=20 A/s for SMCT1 coil, based on its training results in SMCTM1a (point A in the plot).



**Fig. 9.** Load lines (LLs)  $B_{max}/I$  for SMCT1 coil in 2-layer SMCTM1a and for MDP03 and SMCT1 coils in 4-layer SMCTM1b as well as expected  $I_q(B)$  curve for SMCT1 coil based on SMCT1 coil training results in SMCTM1a.



**Fig. 10.**  $B_{max}$  in the aperture and in the inner ( $B_{max}$ -IC) and outer ( $B_{max}$ -OC) coils of dipole magnet MDPCT1 and in the inner (MDP03) and outer (SMCT1) coils of the dipole mirror magnets SMCTM1a/b at 1.9 K.

The data in Fig. 9 suggest that the performance of the dipole mirror SMCTM1b was not limited by the SMCT1 coil since its conductor limit at 20 A/s and 1.9 K is ~13.5 T (point B). The possible causes of quench performance limitations of SMCTM1b are being analyzed.

Figure 10 shows the maximum field  $B_{max}$  achieved in MDP03 and SMCT1 coils of the dipole mirror magnets SMCTM1a/b at 1.9 K. For comparison,  $B_{max}$  in the aperture and in the inner  $(B_{max}\text{-}IC)$  and outer  $(B_{max}\text{-}OC)$  coils of the record dipole magnet MDPCT1 tested in 2020 [3], [4] are also presented. Horizontal dashed lines display the present record fields in accelerator dipole aperture at 4.5 K and 1.9 K, as established by MDPCT1. The maximum field level in MDPCT1 dipole was limited by an outer coil, which also had a 123-mm aperture but did not use stress management structural elements. In the dipole mirror SMCTM1b, the 123-mm aperture SMCT1 coil with stress management, which was made of a similar cable, reached a  $B_{max}$  of 12.6 T. It is more than 1.5 T higher and represents the present record field value for 123-mm aperture dipole coils. The inner

MDP03 coil, previously used in the MDPCT1 dipole, in SMCTM1b mirror reached  $B_{max}$  of 14.5 T. This is lower than the record coil  $B_{max}$  in MDPST1 and the SMCTM1b mechanical limit by only 0.5 T or ~3%.

# V. CONCLUSION

The SMCT coil concept has been proposed and is being studied at Fermilab for high-field and/or large-aperture accelerator magnets made of low-temperature and high-temperature superconductors. The SM structure is used to provide precise coil geometry, reduce coil deformations under large Lorentz forces and limit the excessively large strains and stresses in the coil.

The first 123-mm aperture Nb<sub>3</sub>Sn SMCT1 dipole coil was designed and built at Fermilab to validate and study the SM coil concept and performance. The SMCT1 coil was tested in two dipole mirror configurations.

In the first test, after training, the SMCTM1a mirror magnet with the SMCT1 coil powered individually, has reached a  $B_{max}$  in the coil of 12.7 T at 1.9 K and 12 T at 4.5 K. This corresponds to ~90% of its SSL and is a record field for accelerator dipole coils of this size. The observed reduction of the coil  $B_{max}$  with respect to the SSL at both 1.9 K and 4.5 K is very likely due to conductor degradation during coil fabrication and mirror assembly. After TC the magnet re-training started at 11.2 T, showing poor training memory. However, no conductor degradation was found after TC. The possible causes of magnet re-training are being studied and effort are being made to improve the next coils.

In the 4-layer SMCTM1b configuration, the  $B_{max}$  reached in SMCT1 coil at 1.9 K was 12.6 T at a  $B_{max}$  in the inner MDP03 coil of 14.5 T. The maximum field in MDP03 coil is close to its mechanical limit of 15 T and to the maximum field reached in the inner coil of the record dipole MDPCT1. The test and data analysis were complicated by the presence of voltage spikes in both coils. The cause of voltage spikes and magnet performance limitations are being investigated and will be addressed in the next magnet test.

The successful development and demonstration of the SMCT coil concept establish a solid basis for large-aperture high-field dipole and quadrupole magnets for Muon Colliders [15] and other applications such as the 2<sup>nd</sup> IR for EIC [16]. Fabrication of the second SMCT coil and its test independently and in two dipole configurations with the SMCT1 coil and MDPCT1 inner coils will allow to further study the potential of SMCT coil technology.

# ACKNOWLEDGMENTS

The authors thank technical staff of Fermilab's Magnet Technology Division for their valuable contributions to magnet development, fabrication, and test.

# REFERENCES

[1] V.V. Kashikhin, I. Novitski, A.V. Zlobin, "Design studies and optimization of high-field Nb<sub>3</sub>Sn dipole magnets for a future Very High Energy pp

- Collider," in Proc. IPAC'17, Copenhagen, Denmark, May 2017, p. 3597. doi:10.18429/JACoW-IPAC2017-WEPVA140
- [2] A.V. Zlobin et al., "Conceptual design of a 17 T Nb<sub>3</sub>Sn accelerator dipole magnet," in Proc. IPAC'18, Vancouver, Canada, Apr.-May 2018, p. 2742. doi:10.18429/JACoW-IPAC2018-WEPML027
- [3] A.V. Zlobin et al., "Development and First Test of the 15 T Nb<sub>3</sub>Sn Dipole Demonstrator MDPCT1", IEEE Trans. on Appl. Supercond., Vol. 30, Issue 4, 2020, doi:10.1109/TASC.2020.2967686
- [4] A.V. Zlobin et al., "Reassembly and Test of High-Field Nb<sub>3</sub>Sn Dipole Demonstrator MDPCT1", IEEE Trans. on Appl. Supercond., Vol. 31, Issue 5, August 2021, doi:10.1109/TASC.2020.2967686
- [5] D.R. Chichili et al., "Design, Fabrication and Testing of Nb<sub>3</sub>Sn Shell Type Coils in Mirror Magnet Configuration", CEC/ICMC 2003, Alaska, September 22-25 2003. AIP Conf. Proc. 710, 775 (2004), http://dx.doi.org/10.1063/1.1774754
- [6] A.V. Zlobin et al., "Testing of Nb<sub>3</sub>Sn quadrupole coils using magnetic mirror structure", CEC/ICMC'2009, Tucson, AZ, 2009. AIP Conf. Proc. 1218, 1031 (2010); <a href="https://dx.doi.org/10.1063/1.3422262">https://dx.doi.org/10.1063/1.3422262</a>
- [7] A.V. Zlobin, "Cos-theta Nb<sub>3</sub>Sn dipole for a Very Large Hadron Collider", Ch. 7, in Nb<sub>3</sub>Sn Accelerator Magnets – designs, technologies, and performance, eds. D. Schoerling and A.V. Zlobin, Springer, 2019, p. 157
- [8] A.V. Zlobin, "Nb<sub>3</sub>Sn 11 T Dipole for the High Luminosity LHC (FNAL)", Ch. 8, in Nb<sub>3</sub>Sn Accelerator Magnets – designs, technologies, and performance, eds. D. Schoerling and A.V. Zlobin, Springer, 2019, p. 193
- [9] I. Novitski et al., "Development of a 120-mm Aperture Nb<sub>3</sub>Sn Dipole Coil with Stress Management," IEEE Trans. Appl. Supercond., v. 32, no. 6, pp. 1–5, Sep. 2022. doi:10.1109/tasc.2022.3163062.
- [10]I. Novitski et al., "Using Additive Manufacturing technologies in high-field accelerator magnet coils," FERMILAB-CONF-21-369-TD, 2021.
- [11]E. Barzi et al., "Development and Fabrication of Nb<sub>3</sub>Sn Rutherford Cable for the 11 T DS Dipole Demonstration Model", IEEE Trans. Appl. Supercond., v. 22, no. 3, 6000805, Jun. 2012. doi:10.1109/tasc.2011.2180869
- [12] I. Novitski et al., "Design and Assembly of a Large-Aperture Nb<sub>3</sub>Sn Cos-Theta Dipole Coil with Stress Management in Dipole Mirror Configuration," IEEE Trans. on Appl. Supercond., Vol. 33, Issue 5, 2023, 4001405, doi: 10.1109/TASC.2023.3244894
- [13] I. Novitski et al., "Development and test of a large-aperture Nb₃Sn costheta dipole coil with stress management," IEEE Trans. on Appl. Supercond., Vol. 34, Issue 5, 2024, 4001305, doi: 10.1109/TASC.2023.3344424
- [14] A.V. Zlobin et al., "Development and test of a large-aperture Nb<sub>3</sub>Sn costheta dipole coil with stress management," in Proc. IPAC2024, Nashville, Tennessee, May 2024, p. 2858, doi:10.18429/JACoW-IPAC2024-WEPS68
- [15]L. Bottura et al., "Magnets for a Muon Collider Needs and Plans," IEEE Trans. on Appl. Supercond., Vol. 34, Issue 5, 2024, 4005708, doi: 10.1109/TASC.2024.3382069.
- [16]A.V. Zlobin et al., "Feasibility Study of Large-Aperture High-Field Nb<sub>3</sub>Sn Magnets for the 2<sup>nd</sup> EIC Interaction Region," in Proc. IPAC'23, Venice, Italy, May 2023, p. 3716, doi:10.18429/JACoW-IPAC2023-WEPM063